frontiers in Marine Science

ORIGINAL RESEARCH
published: 10 August 2021
doi: 10.3389/fmars.2021.677632

Phytoplankton Increase Along the Kuroshio Due to the Large Meander

Daniel Andres Lizarbe Barreto[1]*, *Ricardo Chevarria Saravia*[1], *Takeyoshi Nagai*[2] and *Takafumi Hirata*[3]

[1] Facultad de Pesquería, Universidad Nacional Agraria La Molina, Lima, Peru, [2] Department of Ocean Sciences, Tokyo University of Marine Science and Technology, Tokyo, Japan, [3] Arctic Research Center, Hokkaido University, Sapporo, Japan

The Kuroshio Large Meander (LM) is known to be highly aperiodic and can last from 1 to 10 years. Since a stationary cold core formed between the Kuroshio and the southern coast of Japan off Enshu-Nada and approaching warm saltier water on the eastern side of the LM changes the local environment drastically, many commercially valuable fish species distribute differently from the non-LM period, impacting local fisheries. Despite this importance of the LM, the influences of the LM on the low trophic levels such as phytoplankton and zooplankton have still been unclear. In this study, satellite daily sea surface chlorophyll data are analyzed in relation to the LM. The results show positive anomalies of the chlorophyll-a concentration along the Kuroshio path during the LM periods, 2004–2005 and 2017–2019, from the upstream off Shikoku to the downstream (140°E). These positive anomalies are started by the triggering meander generated off south of Kyushu, which then slowly propagates to the downstream LM region in both the LM periods. Even though the detailed patterns along the Kuroshio region in the two LM periods were different, similar formations of the positive anomalies on the western side of the LM with shallower mixed layer depth are observed. Furthermore, we found clear relationships between the minimum distance from several stations along the coast to the Kuroshio axis and the mean chlorophyll-a anomaly, with significant correlations with the distance from different stations.

Keywords: phytoplankton, eddy re-stratification, remote sensing, submesoscale eddies, Kuroshio large meander

OPEN ACCESS

Edited by:
Hiroaki Saito,
The University of Tokyo, Japan

Reviewed by:
Sachihiko Itoh,
The University of Tokyo, Japan
Antonio Bode,
Spanish Institute of Oceanography, Spain

***Correspondence:**
Daniel Andres Lizarbe Barreto
20141316@lamolina.edu.pe

Specialty section:
This article was submitted to Coastal Ocean Processes, a section of the journal Frontiers in Marine Science

Received: *08 March 2021*
Accepted: *05 July 2021*
Published: *10 August 2021*

Citation:
Lizarbe Barreto DA, Chevarria Saravia R, Nagai T and Hirata T (2021) Phytoplankton Increase Along the Kuroshio Due to the Large Meander. Front. Mar. Sci. 8:677632. doi: 10.3389/fmars.2021.677632

1. INTRODUCTION

The Kuroshio south of Japan is known to exhibit a characteristic path bimodality, switching between relatively straight paths and a meandering one (Masuda, 1982; Kawabe, 1985). This different types of path (bimodal feature) cannot be found in other western boundary currents. Uda (1937) was the first to report the abnormally cold water temperature in the stationary cold core formed off Enshu-Nada (137–139°E, see **Figure 1A**) by the Kuroshio Large Meander (LM). The LM is considered to have important effects on storm tracks, extratropical cyclone activities, and local precipitations (e.g., Xu et al., 2010; Nakamura et al., 2012; Hayasaki et al., 2013), as well as an influence on local fishery activities (Uda, 1937), marine resources and ship navigation (Kawabe, 1995; Liu et al., 2018). Therefore, extensive studies have been carried out to understand the mechanisms of the formation and the decay of the LM. Earlier studies using limited *in-situ* observation data provided several hypotheses on the formation of the LM, such as the Oyashio intrusion, El Niño variability, and solar activities (see Stommel and Yoshida, 1972). Later,

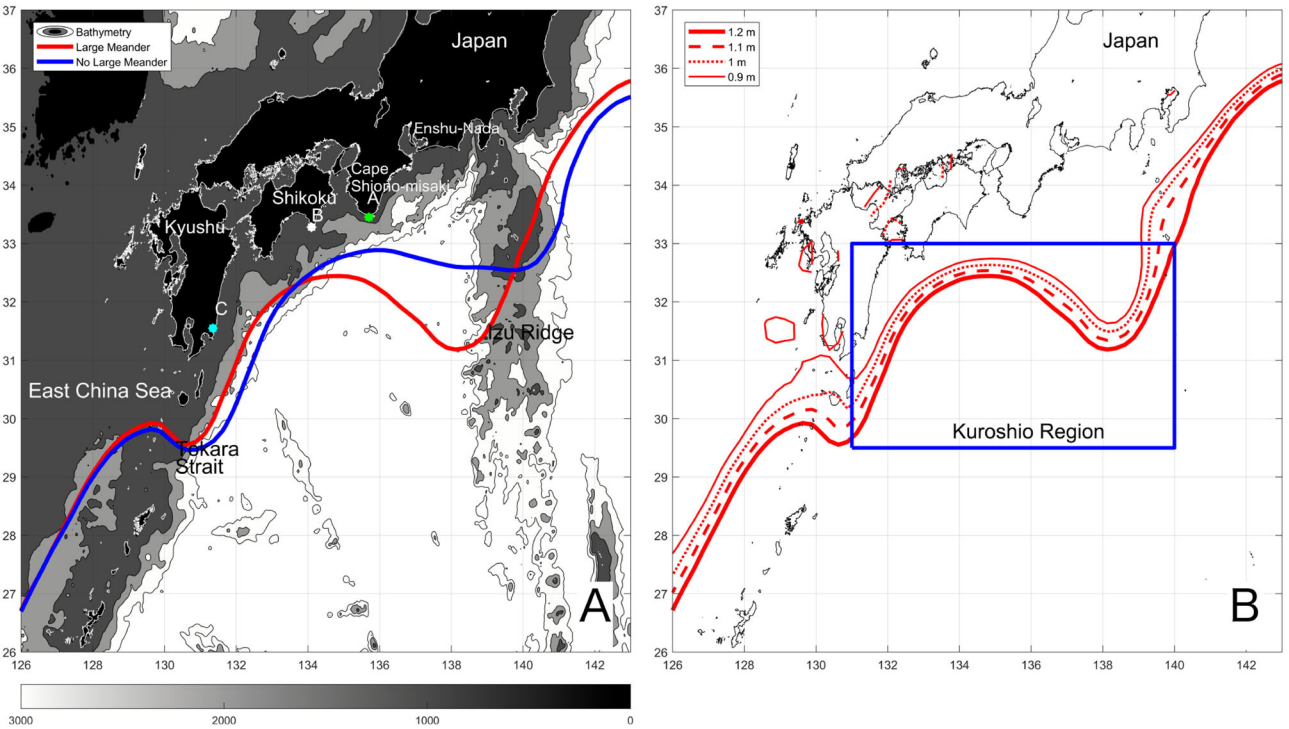

FIGURE 1 | (A) Bimodal paths of the Kuroshio for the No Large Meander (blue line) and the Large Meander (red line) paths. Contours are drawn for the bathymetry with an interval of 1,000 m. **(B)** The Kuroshio axes during the LM defined with the different definitions with SSH values at 1.2, 1.1, 1, and 0.9 m. The blue box represents the Kuroshio region, in which the path length, chlorophyll-a, mixed layer depth, and wind stress are extracted along the Kuroshio axes.

Kawabe (1985, 1986, 1987, 1995) found that the Kuroshio path modulations can be detected by tidal height data along the Kii Peninsula (136°E in **Figure 1A**), and Hachijojima Island (∼33°N, ∼140°E), and that slight north-south shifts of the Kuroshio paths in the upstream Tokara regions (**Figure 1A**) could lead to the formations of the LM or the non-Large Meander (NLM). In addition to the *in-situ* observations, idealized regional numerical models have been utilized to investigate the formation mechanisms of the LM (e.g., White and McCreary, 1976; Chao, 1984; Yasuda et al., 1985; Akitomo et al., 1991). These regional scale numerical studies have reproduced bimodal paths and demonstrated the importance of mesoscale variabilities near the jet. However, to resolve mesoscale eddies with the limited computer power, these simulations needed to be conducted with small size domains. This made impossible to consider the variations in the mesoscale eddy activities caused by the decadal changes in basin scale atmospheric disturbances, that was recently revealed by the satellite altimetry data. These altimetry data have enabled us to identify the mesoscale eddies in a wide area and analyze their roles in forming the LM (Ambe et al., 2004, 2009). The mesoscale eddies are ubiquitous in the ocean. They propagate westward as the first baroclinic mode Rossby waves with swirling water and large thermocline displacements (e.g., Waseda et al., 2002).

The Kuroshio and its downstream, the Kuroshio Extension are known to be rich in these mesoscale eddies (Xu et al., 2010). Previous satellite observations have suggested that the short-term Kuroshio meander and the LM formations are involved with these mesoscale eddies (Waseda et al., 2002; Miyazawa et al., 2004).

The state-of-the-art ocean assimilation and reanalysis studies on the Kuroshio became feasible with these satellite observations. These assimilated data are very useful to capture the processes involved in the Kuroshio path variations (Miyazawa et al., 2005; Kagimoto et al., 2008; Usui et al., 2008) and resolve interactions between mesoscale eddies and the Kuroshio (Ebuchi and Hanawa, 2000, 2003; Ichikawa, 2001; Ambe et al., 2004, 2009). Using one of such ocean assimilation experiments, Usui et al. (2013) and Usui (2019) proposed three necessary conditions to form the LM. First, the Kuroshio Extension has to be in the stable state to maintain the end point of the LM near the coast through the gap north of the Izu Ridge. Second, the low sea surface height anomaly needs to propagate from west to the region off south of Kyushu. Lastly, the positive sea surface height anomaly needs to be formed east of Taiwan. The latter two negative and positive sea surface height anomalies form dipole structures off south of Kyushu to reinforce each other, leading to a formation of a trigger meander that could result in the LM formation.

In addition to the altimetry data, the ocean color satellite remote sensing has enabled us to have a wide view of the chlorophyll-a distributions (e.g., Yamada et al., 2004). Despite

of this, little has been known about the influence of the LM on the surface chlorophyll-a distribution patterns during the LM periods. A previous study by Nakata (1994) has pointed out that the stationary state of the Kuroshio LM may suppress the production of prey for sardine larvae, while the LM in the initial stages may induce upwelling events which may increase the abundance of the prey. These upwelling events can also be expected when cyclonic eddies are generated behind islands in subinertial currents. For example, cyclonic eddies generated by the Kuroshio branch current encountering the Izu Oshima Island have been reported to increase the chlorophyll-a (Kimura et al., 1997). Although the trigger meander of the LM formed south of Kyushu and propagates to the downstream also has cyclonic circulations, it is still unclear whether and how the nutrients are supplied to the surface and what the influences of the cyclonic trigger meander on the lower trophic levels are. In this study, relatively long-term satellite sea surface chlorophyll-a data that include recent two LM events are analyzed. The objective of this research is to clarify the effects of the LM events from its formation and decay including the trigger meanders on the phytoplankton abundance and distribution patterns.

2. DATA AND METHODS

2.1. Kuroshio Data

The Kuroshio Current exhibits a remarkable bimodal feature (also referred to as the Kuroshio path variations) (Taft, 1972): The Non-Large Meander (NLM) path along which the Kuroshio flows along the southern coast of Japan and the Large Meander (LM) path along which the Kuroshio flows far away from the coast off Enshu-Nada (Kawabe, 1987, 1995). In order to differentiate the LM periods, average paths of the LM and the NLM are computed using reprocessed (Jason-3, Sentinel-3A) satellite altimetry data obtained from Copernicus Climate Change Service (C3S) (**Figure 1A**). The average LM path of the Kuroshio defined at sea surface height of 1.2 m is obtained for the last two LM periods (2004–2005 and 2017–2019).

The LM occurrence is highly aperiodic and the LM state can last from 1 to 10 years. During the study period, the Kuroshio south of Japan took the LM path twice. The first LM occurred during the period from August 2004 through August 2005 after a NLM period of 13 years (Miyazawa et al., 2008). Prior to the LM, a trigger meander was generated off southeastern coast of Kyushu in February 2004, which then propagated eastward from south of Shikoku up to Cape Shiono-Misaki in about 4 months (**Figure 1A**, Endoh and Hibiya, 2009). The second LM during the study period is still currently (June 2021) underway since August 2017 (Usui, 2019). After 12 years since the LM 2004–2005 (Nagano et al., 2018), a small meander developed in late March, 2017 southeast of Kyushu Island, propagated eastward to the region off the Enshu-Nada in August, 2017, which was considered to have induced the Kuroshio LM.

2.2. Ocean Satellite Reprocessed Data

Similar to the previous studies (e.g., Qiu and Chen, 2005), the Kuroshio paths were determined by the longest contours at several values of sea surface height. Along these contours, the longitude and latitude are interpolated at a regular distance interval, at which other variables such as chlorophyll-a concentrations, wind stress, and mixed layer depths (MLDs) are interpolated. The range considered for the interpolation is 115–165°E, 22–48°N. Within this region, the data of 4 × 4 km daily chlorophyll-a satellite data obtained from Ocean Color reprocessed L4 (Cloud Free) observations-CMEMS, 0.25 × 0.25 degree resolution monthly mixed layer depth obtained from MERCATOR GLORYS12V1 REANALYSIS-CMEMS, and 0.25 × 0.25 degree 6 hourly wind stress from CERSAT reprocessed observations-CMEMS within 131–140°E (Kuroshio region) were extracted.

2.3. Data Analysis

First, monthly climatologies (September 1997–January 2019) for chlorophyll-a concentration and mixed layer depth were prepared from the daily data, which were then used to obtain anomalies of these variables. The anomalies were then moving averaged with a 13-month window when they are shown as the time-series. To investigate the differences in spatial patterns between the LM and the NLM periods, the mean chlorophyll-a anomaly and the sea surface height as the plan view were computed for the LM and NLM periods (**Figure 2**). Although the subtraction of the monthly climatology of the chlorophyll-a to compute its anomaly may suppress seasonality, obtained spatial patterns in the chlorophyll-a anomaly could reflect the difference in the number of spring and autumn months during the blooming periods. For this reason, the number of spring and autumn months during the LM and NLM periods were counted and divided by the total number of months (**Supplementary Table 1**). The percentage of the spring months (March–May), which are thought to be the largest bloom in a year, during the LM is found to be <20% of the total, whereas it is more than 25% for the NLM period. On the other hand, it is 29 and 26% for the secondary blooming months in autumn (September–November) for the LM and the NLM periods, respectively. In total, the percentages of spring and autumn months are 48 and 53% for the LM and the NLM periods, respectively, suggesting that overestimation of the chlorophyll-a, if exists, is more expected in the NLM rather than the LM period because the NLM period includes more spring and autumn months.

In this study, the Kuroshio axis was determined by the longest contours of the sea surface height at several different values, 1.2, 1.1, 1.0, and 0.9 m. With the higher sea surface height values, the defined Kuroshio axis tends to appear on the offshore side, and vice versa with the lower values (**Figure 1B**). The path length was measured within the Kuroshio region (131–140°E) and was used to illustrate the LM and NLM periods after performing a 13-month moving average (**Figure 3**).

To investigate the relation between the surface chlorophyll-a concentrations and the MLD, the MLD anomaly was computed using the MERCATOR GLORYS12V1 REANALYSIS-CMEMS. For this, the monthly climatology of MLD was first calculated using the data during 1997–2019, which was then subtracted from the MLD. After performing the 13-month running average,

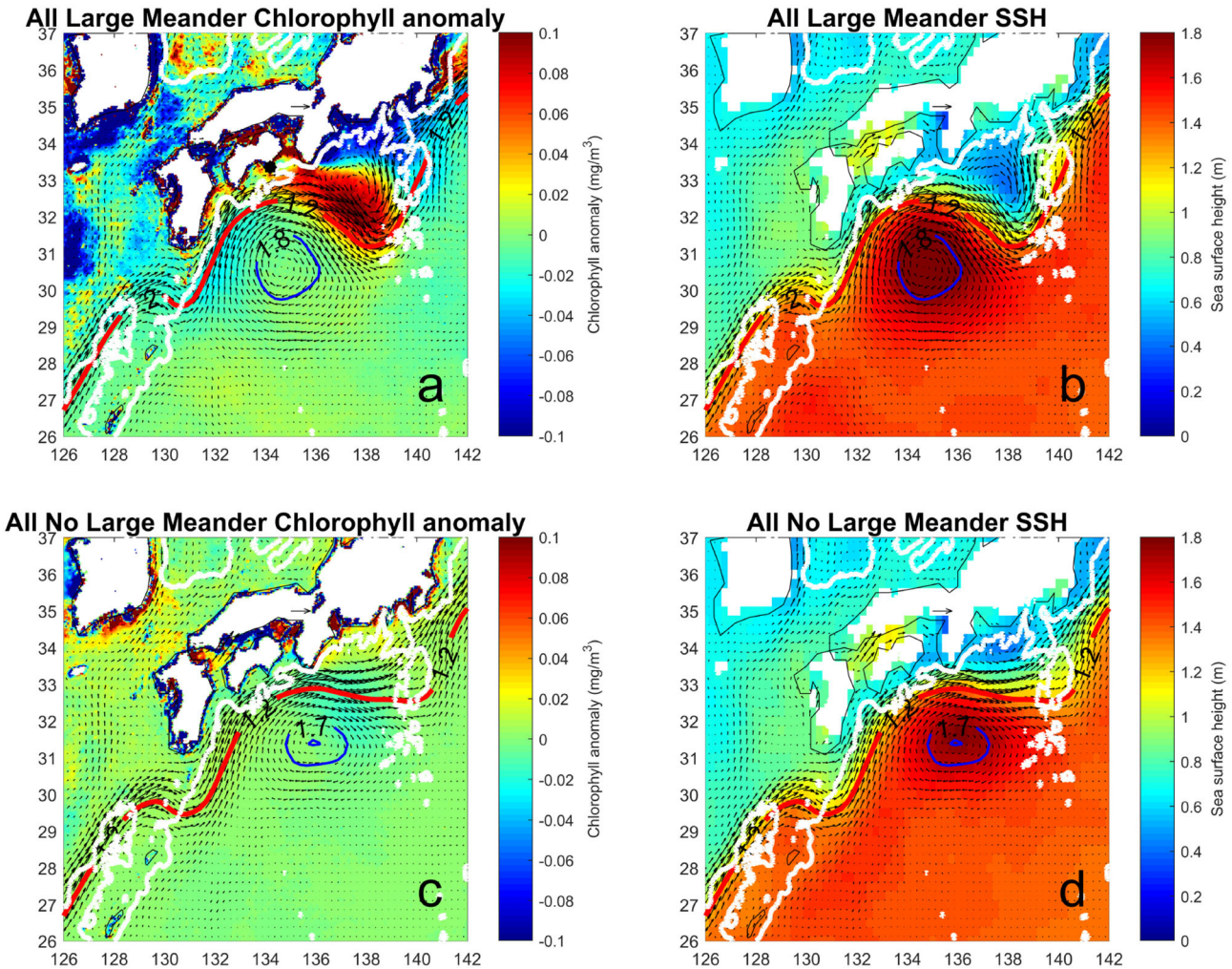

FIGURE 2 | Chlorophyll anomaly and sea surface height (SSH) or absolute dynamic topography during the Large Meander **(a,b)** and No Large Meander **(c,d)**. Geostrophic flow is represented with arrows and a recirculation gyre is illustrated with the blue SSH contours. The red curves represents the Kuroshio axis defined by the SSH contour at 1.2 m.

the MLD anomaly was obtained and compared with the sea surface chlorophyll-a concentrations.

The Pearson correlation coefficient (R) and *P*-value were computed between the physical parameters, such as the mixed layer depth (MLD) or wind stress and the chlorophyll-a anomaly along the Kuroshio axis for the entire period of this study as well as for each LM period (**Supplementary Table 2**). The chlorophyll-a anomaly and the MLD anomaly during the LM periods were extracted during the course of each LM occurrence from its trigger meander through the end, to calculate the Pearson correlation coefficient and the *P*-value. In addition, the Pearson correlation coefficient (R) was computed also between the MLD and the wind stress and shown in **Supplementary Table 3** for the entire period of the study.

When the Kuroshio takes the LM path, the quasi stationary large cyclonic eddy like meander with the doming isopycnal structure is formed off Enshu-Nada, which may lift up the nutrient rich deep water. The influence of the doming nutricline on the phytoplankton, is therefore, likely to appear within the region between the Kuroshio with this cyclonic meander and the coast. Thus, an area off Enshu-Nada within the cyclonic meander (**Supplementary Table 4**) was chosen to identify the effect of the LM on the chlorophyll-a anomaly. Note that the area close to the shore was excluded from the analysis to avoid including the overestimated chlorophyll-a concentrations due to CDOM (colored dissolved organic matter).

To compare the average chlorophyll-a anomaly within the area with the distances between the Kuroshio axis and the coast, several stations such as at Cape Shiono-Misaki (A), Shikoku (B), and south of Kyushu (C) were selected (**Figure 1A**, **Supplementary Table 4**), similar to Kawabe (1995). The minimum distance between the Kuroshio axis defined with the SSH at 1.2 m and each station was computed. In addition to the minimum distance, the maximum value of the SSH was

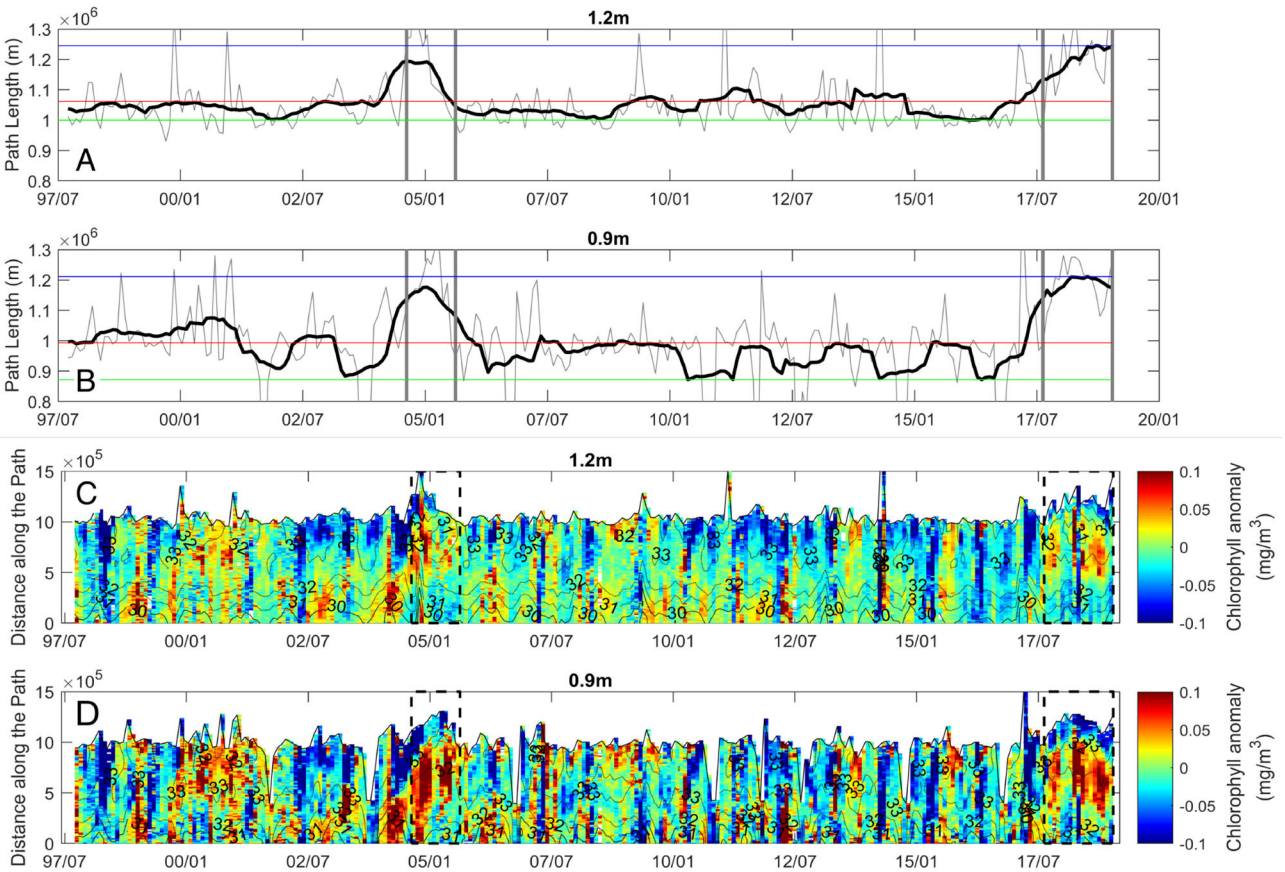

FIGURE 3 | The Kuroshio path lengths within the Kuroshio region (131–140°E) defined in the **Figure 1A** as a blue box with different SSH values for the Kuroshio definition, for **(A)** 1.2, and **(B)** 0.9 m of SSH values. Black lines show the path lengths after 13-month running average of the monthly data, which are shown as the gray lines. The periods indicated with the gray lines represent the large meander periods. Red line indicates the average path length, and blue line the maximum and green line the minimum path length. Chlorophyll anomaly in color as a function of time and path length (distance along the Kuroshio path) with different definitions of the Kuroshio axis with the SSH values for **(C)** 1.2 and **(D)** 0.9 m. Black dashed line indicates the large meander periods. Gray shaded thin line indicates the Path length. The contours are avergae latitude.

computed within the region 130–140°E, 28–35°N, where the center of the anticyclonic recirculation gyre off Shikoku appears. These variables, such as average chlorophyll-a concentrations within the cyclonic meander off Enshu-Nada, the minimum distances, and the maximum SSH values were 13-month running averaged before computing the Pearson correlation coefficients (R) and *P*-values (**Supplementary Table 5**).

3. RESULTS

3.1. The Kuroshio Large Meander and Sea Surface Chlorophyll-a

The average LM path is found to be closer to the continental shelf in Kyushu (Station C in **Figure 1A**) than that during the NLM period, which is contradict to what suggested by Kawabe (1985, 1995) showing based on the tidal gauge data that the NLM Kuroshio flows closer to the coast. During the last two large meander periods, latitudes of the Kuroshio path may not fall below 31°N within the Kuroshio region and over the Izu Ridge.

To illustrate the difference in phytoplankton distribution between the LM and the NLM periods, the chlorophyll-a anomaly and the SSH are averaged during the entire LM (**Figures 2a,b**) and NLM (**Figures 2c,d**) periods. The positive chlorophyll-a anomaly extending southeastward from off Shikoku is seen during the LM period, which is absent in the NLM period indicating that the chlorophyll-a concentrations are higher during the LM than the NLM period along the Kuroshio south of Enshu-Nada (**Figures 2a,c**). The enhanced chlorophyll-a concentrations seem to be advected from southeast of Shikoku and Cape Shiono-Misaki to the downstream region, which corresponds to the region near the cyclonically meandering LM path from the meander crest to the trough. The values of this positive chlorophyll-a anomaly are found to be much greater than the standard errors (**Supplementary Figure 1**). On the other hand, in the near shore regions off Enshu-Nada, negative chlorophyll-a anomalies are observed during the same LM period. Blue contours of SSH at 1.8 m (**Figures 2a,b**) and 1.7 m (**Figures 2c,d**) represent the anticyclonic recirculation

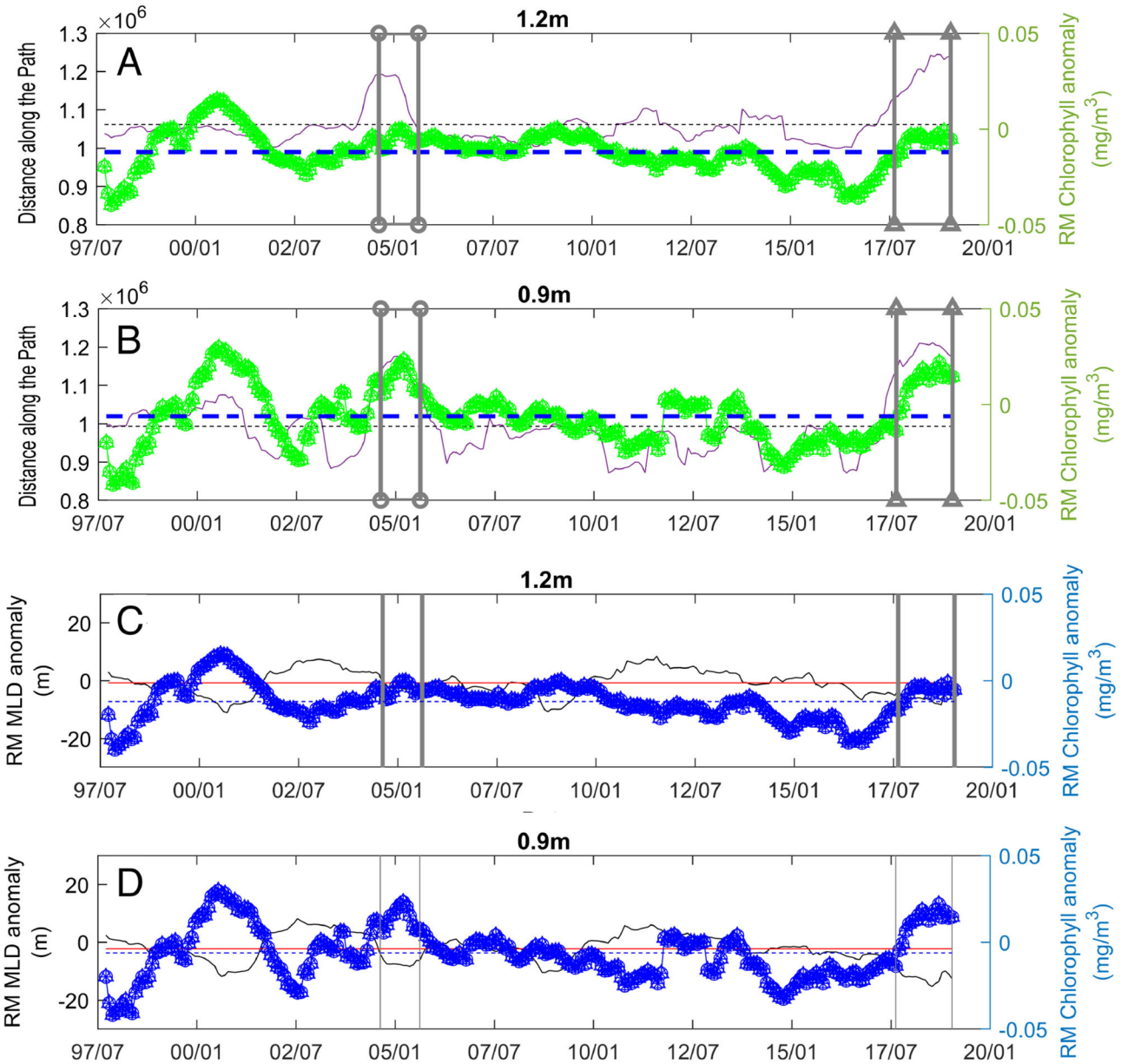

FIGURE 4 | Time series of the 13-month running-mean path length (magenta line) and the chlorophyll anomaly (green line) with different definitions of the Kuroshio axis with the SSH values for **(A)** 1.2 and **(B)** 0.9 m. Each monthly value is averaged along the path before the running average. Large meander years are enclosed in gray boxes. Blue dashed line indicates the mean chlorophyll anomaly and black dashed line indicates the mean path length. Time series of the 13-month running-mean mixed layer depth in black and chlorophyll-a anomaly in blue along the Kuroshio path with different definitions of the Kuroshio axis with the SSH values for **(C)** 1.2 and **(D)** 0.9 m. Each monthly value is averaged along the path before the running average. Large meander years are enclosed in gray boxes. Red line indicates the average mixed layer depth anomaly. Blue dashed line indicates the average chlorophyll-a anomaly.

gyre off Shikoku, which strengthens and intensifies during the LM periods and plays an essential role in reinforcing baroclinic instability (Usui, 2019). Although a cyclonic circulation is also formed during NLM between the Kuroshio and Enshu-Nada (**Figures 2c,d**), the strength of the circulation is much weaker than that during the LM. To evaluate the effects of the Kuroshio LM on the sea surface chlorophyll-a quantitatively, the LM formation and decay are tracked by measuring the Kuroshio path length within the Kuroshio region (131–140°E, **Figure 1B**) similar to (Usui, 2019). For these analyses along the Kuroshio path, the Kuroshio axis is defined with the longest contour of SSH at four different values. The 13-month running averaged path lengths are found to show larger values than their average path length since the occurrence of the LM triggering meander south of Kyushu (**Figures 3A,B**). After several months, the path lengths increased until they reach $\sim 1.2 \times 10^6$ m. The increase of

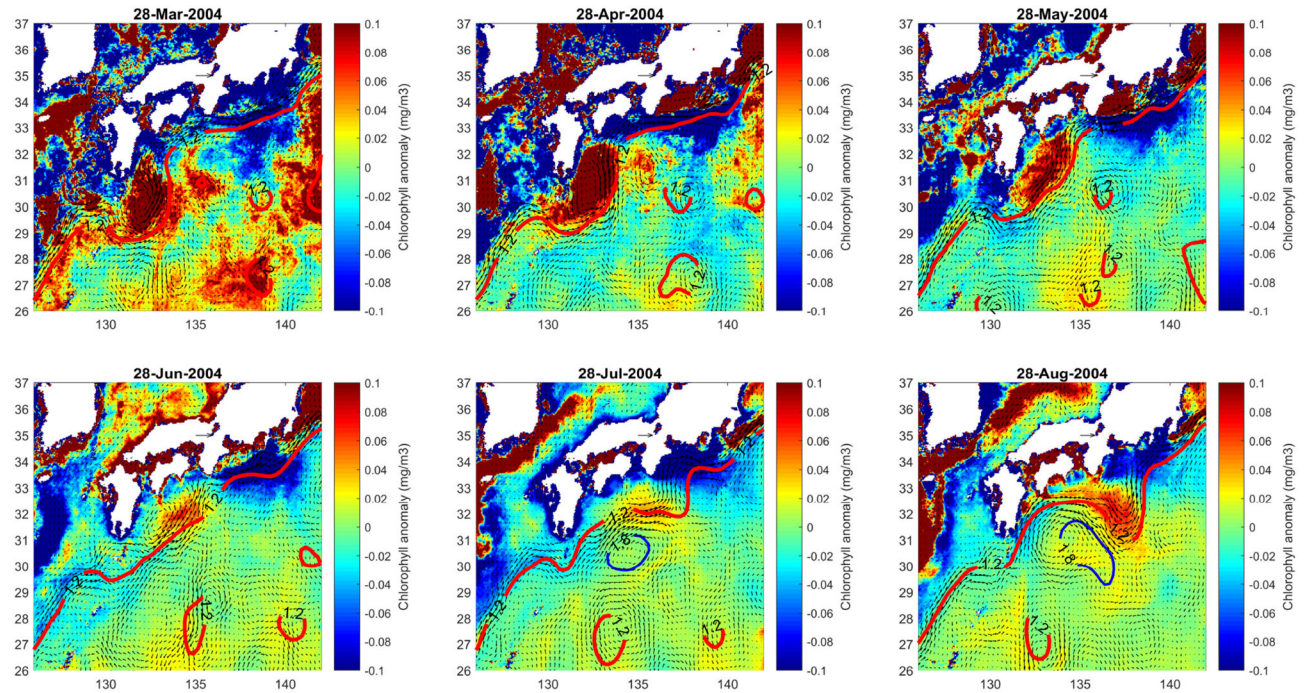

FIGURE 5 | The positive chlorophyll anomaly propagation from the south of Kyushu to the LM trough during the LM formation during the LM 2004–2005.

the path length for the LM since August 2017 seems to be more gradual taking several years to reach $\sim 1.2 \times 10^6$ m than that during August 2004 and 2005. Besides the path length increase during these two LM periods, there seems to be interseasonal and interannual modulations in the path lengths. The former can be seen for the entire time series that can be attributed to the mesoscale variability, and the latter is observed during the NLM periods.

The chlorophyll-a anomaly along two Kuroshio axes (**Figures 3C,D**) is extracted and shown as a function of time and distance along the path from the westernmost longitude of the Kuroshio region, 131°E. Although the patterns of the chlorophyll-a distributions along the axes are similar regardless of the definitions of the axis, the chlorophyll-a anomalies during the LM show somewhat smaller positive anomaly with the axis defined at higher SSH values, for example, at 1.2 m, which corresponds to the offshore most path (**Figure 3C**). On the other hand, the higher positive anomaly during the LM period is found with the axes closer to the coast with the lower SSH values (**Figure 3D**). The results with all the SSH values to define the Kuroshio axis are shown in **Supplementary Figure 2**. These positive anomaly values during the LM seem to propagate from the upstream toward the downstream along the path. The propagation during 2004–2005 is clearer than that of the LM 2017-present. Average chlorophyll anomalies along the Kuroshio axis within the Kuroshio region show that as the meander grows, the positive chlorophyll anomaly increases (**Figures 4A,B**) with values above their means (blue dashed line). This positive anomaly increase is particularly clearer when the average is computed along the Kuroshio with the definition of SSH at 0.9 m. Although the period during 2001–2002 is not defined as the LM period, the large positive anomaly is accompanied by the relatively longer path length in the same period. The correlation coefficient computed between the chlorophyll-a anomaly for the entire time series during 1997–2019 and the path length with the Kuroshio axis defined by the SSH at 0.9 m is as high as $R = 0.57$. The relatively high correlation coefficient suggests that the LM development leads to the phytoplankton increase. It should be noted that the correlation coefficient decreases when computed for the same variables along the Kuroshio axis but defined with the higher SSH values, suggesting that the chlorophyll-a increase on the shore side of the front is more tightly linked with the LM.

3.2. Propagation of Positive Chlorophyll-a Anomaly in Large Meander Periods

During the LM 2004–2005, chlorophyll-a anomaly off south of Kyushu started to increase in February 2004. After a month, on March 28, 2004, the positive chlorophyll anomaly slightly moved northeastward to the region off southeast of Kyushu (**Figure 5**). The initial increase of the positive anomaly coincides with a trigger meander formation south of Kyushu, which is accompanied by a cyclonic circulation between the Kuroshio and the coast with increasing chlorophyll-a. The positive anomaly then propagates toward the downstream. Finally, in August–October 2004, the positive chlorophyll-a anomaly reached the farthest part of the LM from the shore, and remained appearing around the distance of 5–10 $\times 10^5$ m as long as the LM continues. The highest positive chlorophyll anomaly is found at 32°N (contours in **Figure 6B**). The speed of the anomaly propagation from south of Kyushu to the Izu-Ogasawara Ridge is estimated

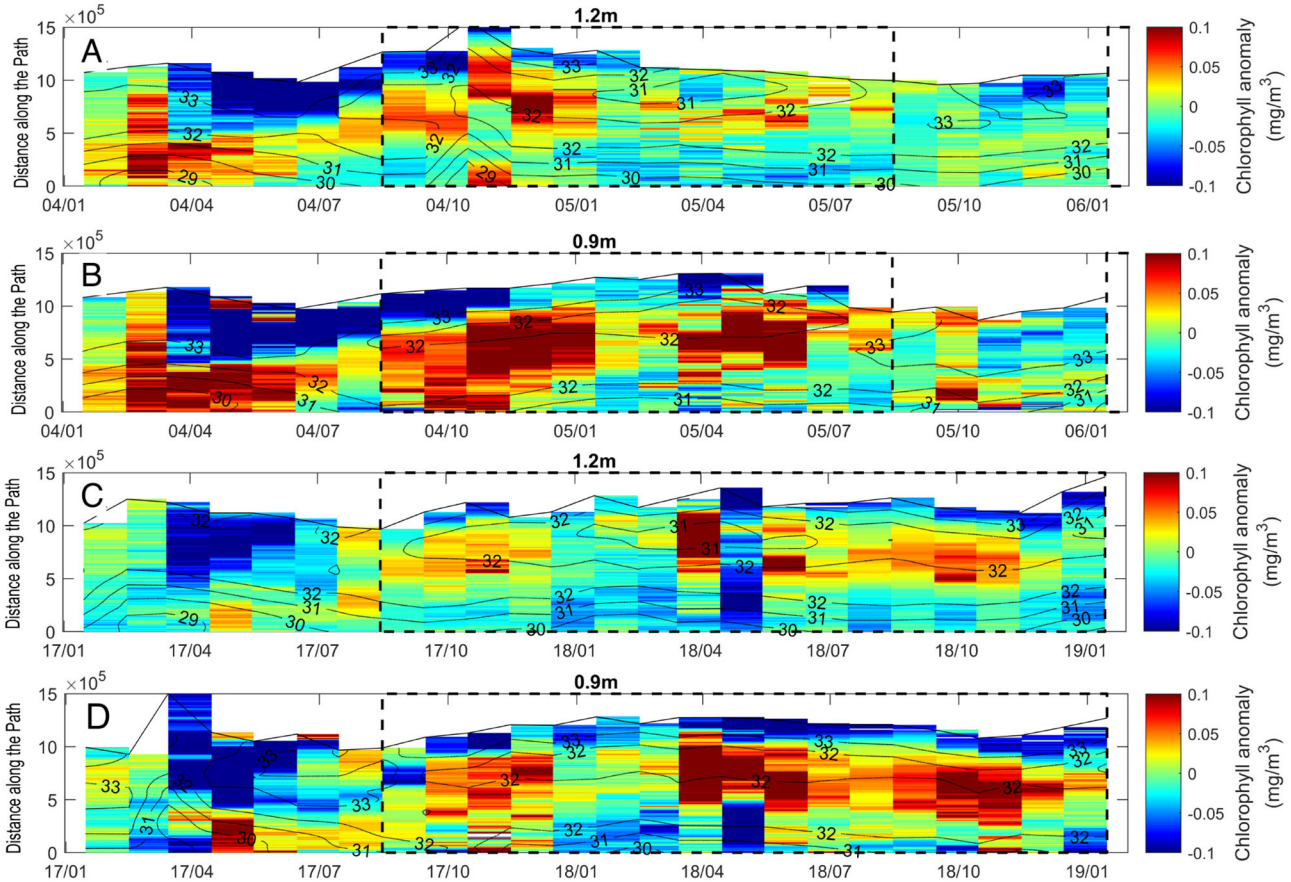

FIGURE 6 | Monthly chlorophyll anomaly extracted during the two large meander periods shown in color as a function of time and distance along the Kuroshio path with different definitions of the Kuroshio axis with the SSH values for **(A,C)** 1.2 and **(B,D)** 0.9 m. **(A,B)** shows LM 2004–2005 and **(C,D)** LM 2017–2019. Black dashed line indicates the large meander periods. Black dotted contour indicates the latitude.

to be 3.0 km day^{-1}, which corresponds to 3.5 cm s^{-1}. This propagation speed is much less than the current speed of the Kuroshio ∼1 ms^{-1}.

The Pearson correlation coefficient (**Supplementary Table 2**) computed between the path length and the chlorophyll-a anomaly only for the LM 2004-2005 including the trigger meander formation shows much higher value, 0.91 than that computed for the entire period, 0.57. The higher correlation coefficient during the LM period suggests that the chlorophyll-a increase along the Kuroshio is strongly affected by the processes associated with the LM.

A similar propagation pattern is found during the LM 2017-present with a trigger meander generated in the end of March 2017, which then propagated toward the downstream region with a similar propagation speed. However, the value of the positive anomaly is slightly less than that during the LM 2004–2005. The positive anomaly is enhanced later when the relatively higher values reaches 5–10 × 10^5 m and the large anomaly persists until the latest time analyzed in this study (**Figure 6B**). Similar to the previous LM 2004–2005, the highest concentration of chlorophyll-a anomaly along the path is found at 32°N (**Figure 6**) on the southwest side of the cyclonic circulation of the LM (**Figure 2a**). The LM grows bigger on average reaching 1.25 × 10^6 m of the running averaged path length during the LM 2017-present compared to the LM 2004–2005 with the path length <1.2 × 10^6 m. The correlation coefficient computed between the path length and the chlorophyll-a anomaly for the LM 2017-present shows also high values with both the definitions for the Kuroshio axis of SSH = 1 m (0.95) and 0.9 m (0.84).

3.3. Mixed Layer Depth and Chlorophyll-a Anomalies Along the Kuroshio

The persistent positive chlorophyll-a anomaly during the LM periods along the Kuroshio could be induced by deeper mixed layer depths (MLDs) that can entrain nutrient rich lower layer water into the surface layers. Interestingly, the 13-month running average MLD shows opposite trend with the chlorophyll-a along the path for the entire period of the analysis (**Figures 4C,D**), suggesting that the positive chlorophyll-a anomaly is associated with the shallower mixed layer depth. The correlation coefficient between the MLD anomaly and chlorophyll-a anomaly shows a negative value of −0.53 with the Kuroshio axis definition of SSH = 0.9 m (**Supplementary Table 2**). When the data are

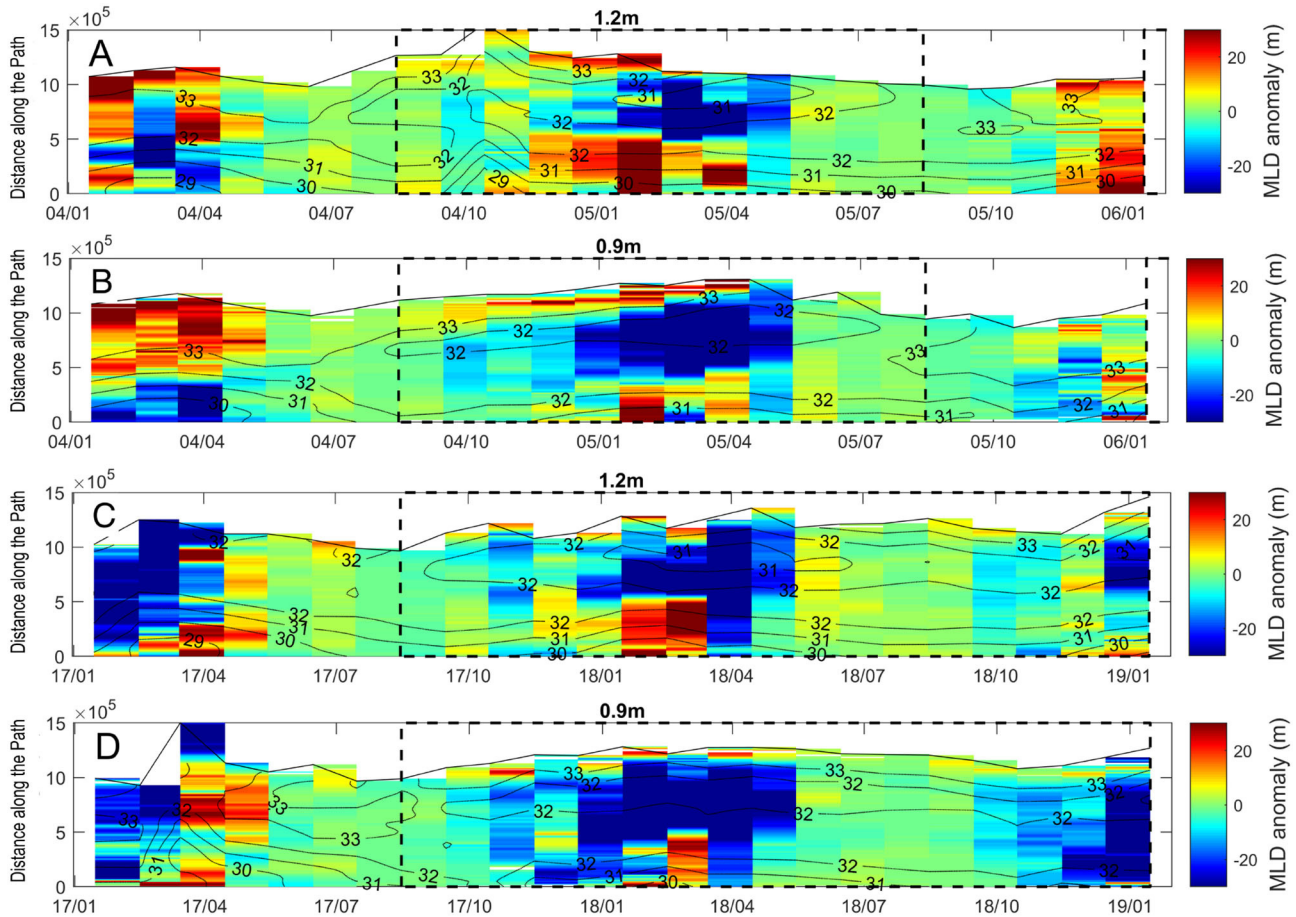

FIGURE 7 | Monthly mixed layer depth anomaly extracted during the two large meander periods shown in color as a function of time and distance along the Kuroshio path with different definitions of the Kuroshio axis with the SSH values for **(A,C)** 1.2 and **(B,D)** 0.9 m. **(A,B)** shows LM 2004–2005 and **(C,D)** LM 2017–2019. Black dashed line indicates the large meander periods. Black dotted contour indicates the latitude.

extracted only for the LM 2004–2005, the MLD and chlorophyll-a anomaly show an even stronger negative correlation with $R = -0.79$. Also for the LM 2017-present, the correlation coefficient is −0.86 with the Kuroshio axis definition at SSH = 1 m (**Supplementary Figure 3C**).

The MLD anomaly as a function of time and distance along the path during the LM 2004–2005 shows that the MLD is shallow along the path where the LM occurs. The clearer negative MLD anomaly during the LM 2004–2005 is seen with the smaller SSH values for the definition of the Kuroshio axis, suggesting that shoaling of the MLD occurs more on the cold side of the front. The latitude range of the MLD shoaling is between 31 and 32°N (contour in **Figure 7**) which coincides with that of the positive chlorophyll-a anomaly during the LM (**Figure 2a**). However, unlike the chlorophyll-a anomaly, the negative anomaly of the MLD does not show clear propagation patterns toward the downstream (**Figure 7**).

Similar mixed layer variations along its path are found also during the LM 2017-present (**Figures 7C,D**). The negative MLD anomaly during the LM 2017-present is also clearer with the smaller SSH values along the Kuroshio axis, i.e., on the dense or cold side of the front. In the 2 year period shown in **Figures 7C,D**, there appears to be a seasonal shoaling of the MLD from autumn to spring. This seasonal MLD variation is, however, less clear during the LM 2004–2005 (**Figures 7A,B**). It should be noted that even after removing seasonality with 13-month running mean, the tendency to have shallow MLD during both the LM periods still remains (**Figures 4A–D**, lower). Wind stress on the surface of the ocean is one of the major forcing mechanisms to cause changes in the MLD. As oppose to the clearer negative MLD anomaly found on the dense side of the front, the higher correlation coefficients between wind stress and MLD are found with higher SSH values for the Kuroshio axis definition. The highest correlation coefficient is 0.51 on the less dense side of the front, which becomes as low as 0.18 on the dense side, where the MLD shoals. These results suggest that the shoaling of the MLD on the dense side of the front is not caused by the weak wind (**Supplementary Table 3**).

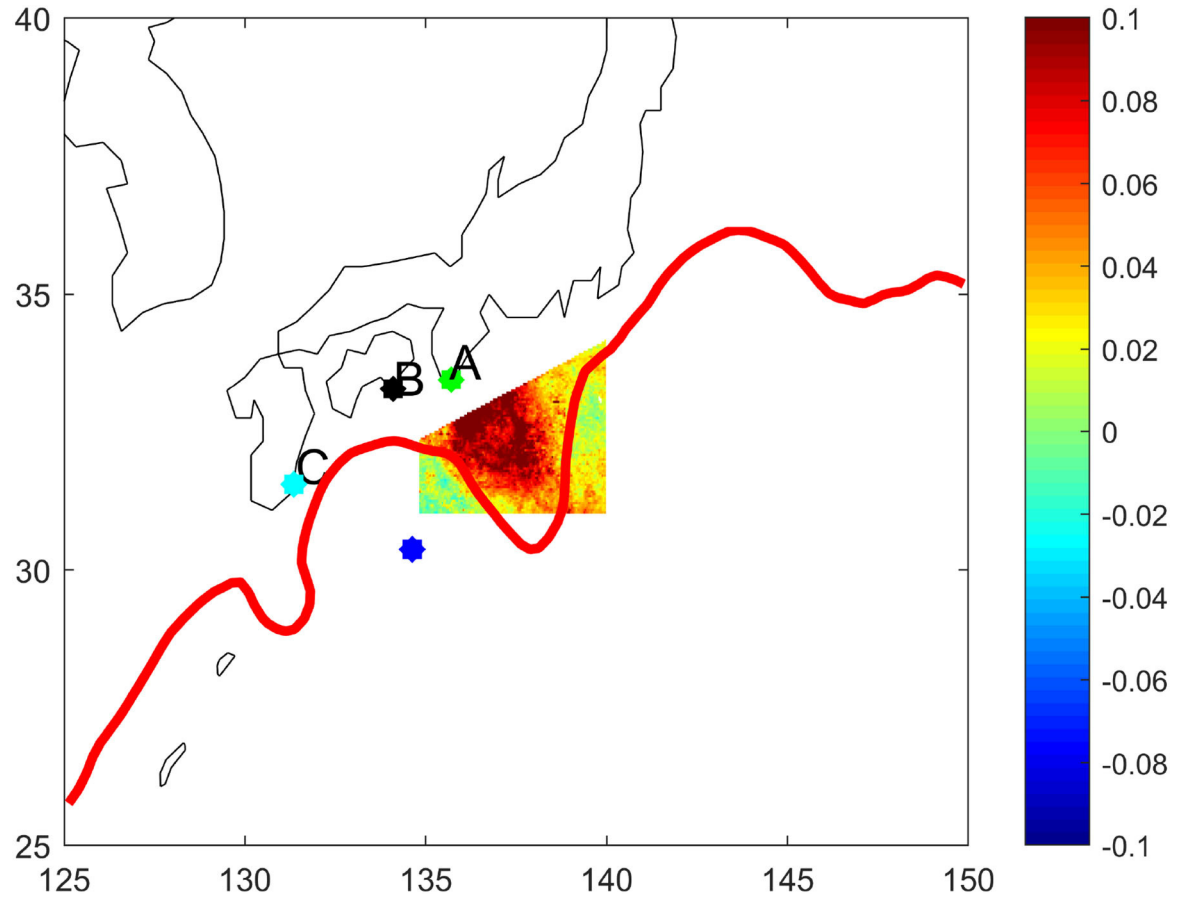

FIGURE 8 | Selected area for representing the LM chlorophyll-a anomaly in color shading and three coastal stations in Cape Shiono-Misaki (A), Shikoku (B), and south of Kyushu (C). Red contour indicates the Kuroshio axis defined with the SSH value at 1.2 m. Blue dot shows an example of the SSH maximum within the recirculation gyre.

3.4. Minimum Distance Between the Kuroshio and the Coastal Stations

It is well-known that an anticyclonic recirculation gyre off Shikoku plays an important role in the LM formation process, as the baroclinic instability near the recirculation gyre south of the small trigger meander slowly propagating eastward grows to the LM (Miyazawa et al., 2008; Usui et al., 2008; Usui, 2019). Also, Mitsudera et al. (2001) reported that the Kuroshio meander grows as the anticyclonic eddy strengthens off the Kii Peninsula (Shiono-Misaki) and decays when the eddy detaches. To investigate the relation among chlorophyll-a anomaly within the LM, the minimum distances between the Kuroshio and the coastal stations, and the strength of the anticyclonic re-circulation, an area within 134.8–140°E, 31–35.5°N is selected (**Figure 8**) to average the surface chlorophyll-a within the LM. The minimum distances between three stations, (A) Cape Shiono-Misaki, (B) Shikoku, and (C) south of Kyushu and the Kuroshio defined as the SSH value of 1.2 m are measured (**Figure 8**, **Supplementary Table 4**). Also, the maximum value of SSH within the recirculation gyre south of Shikoku is examined.

Figure 9B shows that the minimum distance from the station C to the Kuroshio decreases during both the LM periods, indicating that during the LM, the Kuroshio flows closer to the continental shelf southeast of Kyushu near the station C. On the other hand, the minimum distances increase during LM periods for the station A and B. The maximum value of SSH seems to be inversely proportional to the minimum distance from the station C over the long term (**Supplementary Table 5**) with a correlation coefficient, R of −0.73. The correlation coefficient between the minimum distance from the station A and chlorophyll-a anomaly within the selected area calculated during 1997–2019 (January) is found to be high, 0.7145 (**Supplementary Table 5**), reflecting a fact that large distance from the station A to the large meandering Kuroshio coincides with the positive anomaly of the chlorophyll-a. On the other hand, the correlation coefficient between the minimum distance from the station C and chlorophyll-a anomaly shows a negative value, −0.53, suggesting that the more closely flowing Kuroshio to the coast of southeast of Kyushu near the station C during the LM coincides with the positive chlorophyll-a anomaly.

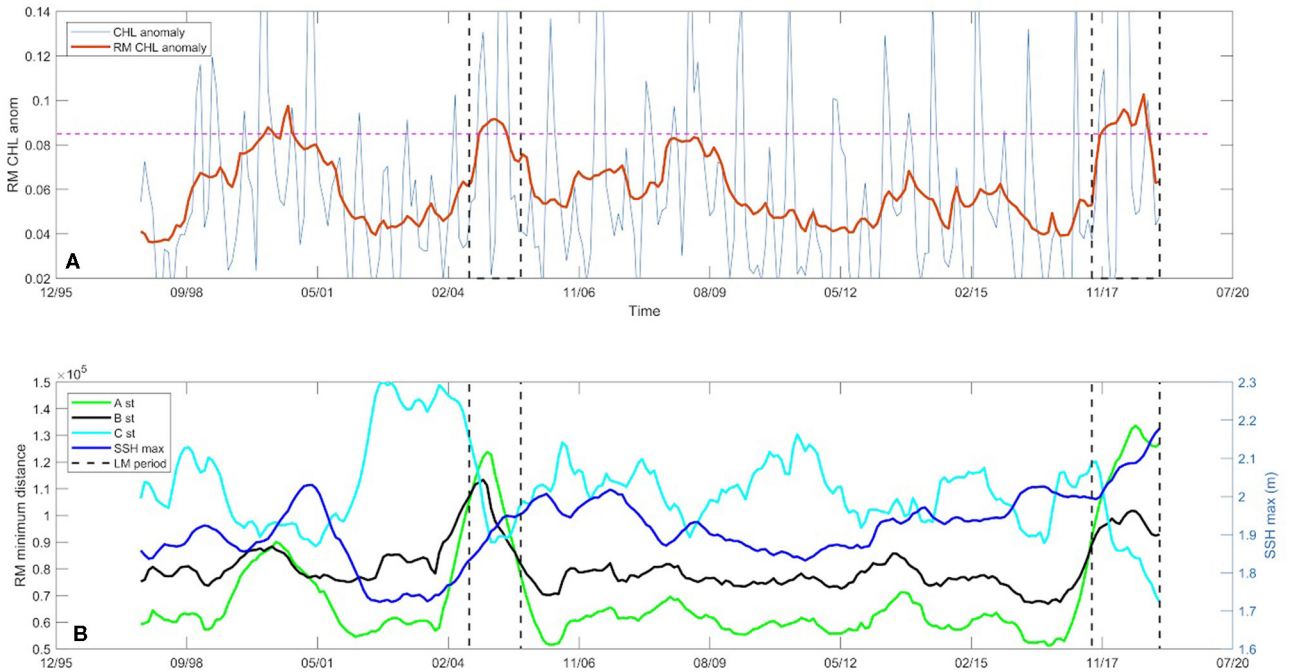

FIGURE 9 | Time series of the 13 month running-mean chlorophyll-a anomaly within the selected area in the LM is shown as red with monthly values in blue line. Black dashed lines indicate the LM periods **(A)**. Time series of the minimum distance from the stations A (green), B (black), and C (cyan) to the Kuroshio axis defined with the SSH value at 1.2 m with a 13-month running average. Blue line indicates the 13 month running mean maximum SSH value in the recirculation gyre **(B)**.

4. DISCUSSION

The mean LM path of the Kuroshio obtained by averaging them during the two LM events, the LM 2004–2005 and the LM 2017-present, shows differences compared to the NLM path not only in the region south of Enshu-Nada, but also southeast of Kyushu (**Figure 1A**). The previous study by Kawabe (1987) has defined the LM and NLM paths, which show that the NLM Kuroshio flows closer to the coast from the upstream Kyushu toward the downstream. In contrast, the mean LM path in this study is closer to the coast than the NLM path in the region southeast of Kyushu (**Figure 1A**). One possible explanation for this discrepancy is that our analyzed period is relatively longer over 20 years than that in Kawabe (1987). Also, as SSH satellite data is only available since 1993, prior LM periods than this could only be studied by SST satellite data and tide gauge data (Kawabe, 1985, 1986, 1987, 1995), which might induce inaccurate estimate on the path position. On the other hand, the recent LM periods analyzed in this study are not as enduring as the LMs studied by Kawabe, which could have also influenced the variability of the path. Nevertheless, the more closely flowing Kuroshio to the continental slope off southeast of Kyushu may induce strong turbulence. A previous observational study using a tow-yo microstructure profiler by Nagai et al. (2019a) showed that near-inertial internal waves trapped within the Kuroshio flowing closely to the continental slope generate large turbulent kinetic energy dissipation rates and associated large nitrate diffusive fluxes in the Hyuga Nada Sea, southeast of Kyushu. The nutrients injected through this mechanism can be advected by the strong Kuroshio flow and provided to phytoplankton in a few hundred kilometers downstream, which would correspond to the region where the positive chlorophyll-a anomaly within the LM. The elevated diapycnal mixing caused by the closely flowing Kuroshio may keep supplying nutrients to primary producers along the Kuroshio. However, the previous observations using an autonomous microstructure profiling float and a BGC float by Nagai et al. (2021) showed that the downstream increase in the chlorophyll-a in response to the nutrient diffusive flux occurred at the subsurface chlorophyll maximum, which can not be observed by the satellite.

On the other hand, the most notable surface chlorophyll-a anomaly during the course of the LM events is always associated with the small cyclonic meander slowly propagating eastward from south of Kyushu to the LM (**Figures 4A,B**, **6**). One of the important elements for the LM formation is this small cyclonic meander appearing south of Kuyshu (Solomon, 1978; Usui, 2019). The Kuroshio axis defined with the SSH value of 0.9 and 1 m are better to track chlorophyll-a propagation during LM periods, suggesting that the propagation occurs on the coastal side of the front, rather than along the main stream of the Kuroshio. The propagation speed of this cyclonic meander is estimated as 3.5 cm s^{-1}. The corresponding time required to travel from south of Kyushu to the region off Enshu-Nada is ∼10 months. This propagation time scale is much longer than the phytoplankton doubling time of ∼1 day, suggesting that observed positive anomaly needs to be sustained by the

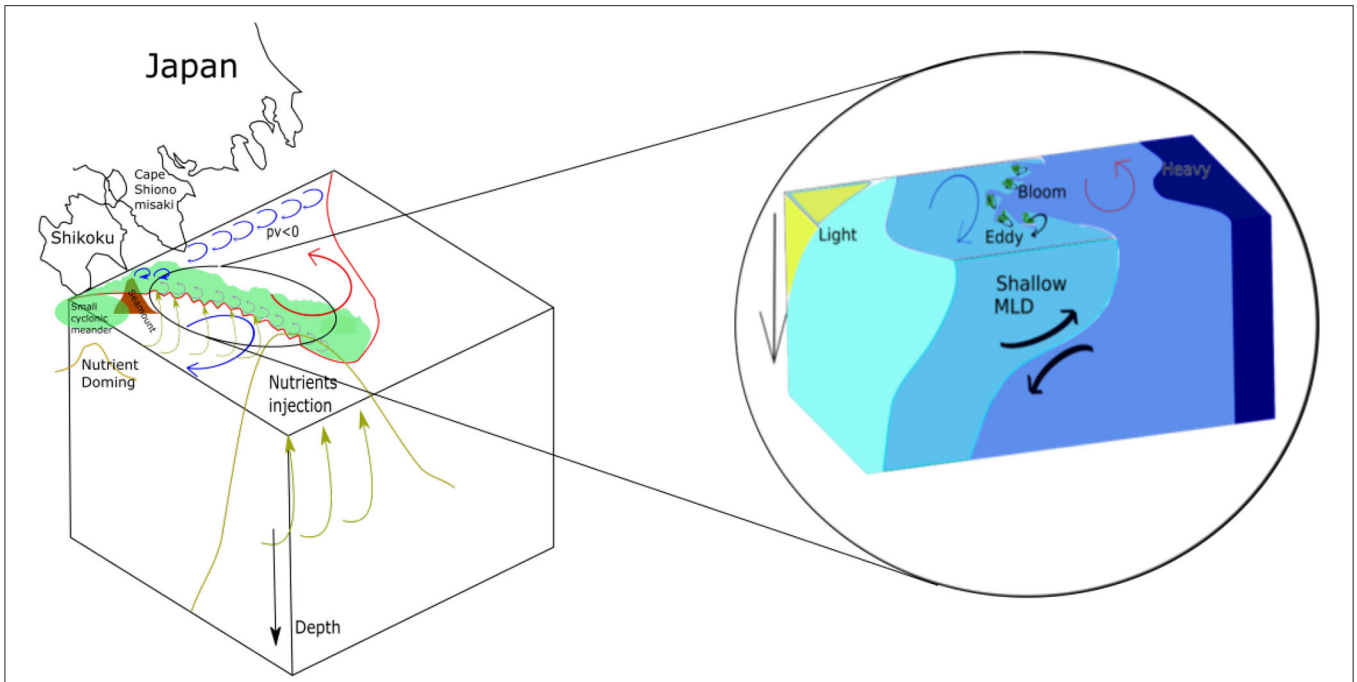

FIGURE 10 | Hypothesis to arise positive chlorophyll-a anomaly in the LM. The small cyclonic trigger meander slowly propagates eastward from the region south of Kyushu, and emerges as the LM off Enshu-Nada. The small cyclonic meander is expected to retain the nutrient doming structure accompanied by the surface chlorophyll-a positive anomaly. As the LM occurs, the Kuroshio flows closer to the coast in the region south of Kyushu, which could induce strong turbulent mixing and nutrient supply (Nagai et al., 2019a). Also, the small seamounts along the Kuroshio, and/or the strong westward counter current along the south coast of Enshu-Nada could produce negative potential vorticity, that can induce turbulence and inject domed subsurface nutrient to the upper layers. The mixed layer restratification seems to increase the phytoplankton on the western part of the LM.

continuous nutrient supply. Also, as the Kuroshio entrains waters from the nearshore regions, the phytoplankton communities within the positive chlorophyll-a anomaly is most likely advected laterally across the front.

During 2000–2001, the chlorophyll-a anomaly rises (**Figures 4A–D**, upper) along the Kuroshio path due to a similar process triggered by a small meander southeast of Kyushu, which did not develop as a LM. It is well-known that mesoscale eddies propagating westward in the Kuroshio recirculation region sometimes impinge on the Kuroshio off the southeast of Kyushu and subsequently a small meander is generated (Ebuchi and Hanawa, 2003; Usui, 2019). The generation of the trigger meander is associated with the supply of cyclonic vorticity at the southern coast of Kyushu (Endoh and Hibiya, 2000, 2001).

One of the turbulence generation mechanisms involved with the Kuroshio besides the near-inertial wave trapping, is the centrifugal instability within the streak of the negative potential vorticity (PV) (Gula et al., 2016). However, when the Kuroshio approaches to the south coast of Japan, the frictional generation of the cyclonic vorticity over the sloping bottom boundary layer does not lead to the negative PV generation. The negative PV generation caused by the Kuroshio south of Honshu is possible when there are seamounts and shills. On the northern slope of these seamounts, the Kuroshio can generate the negative PV leading to the centrifugal instability, which has recently pointed out by Durán Gómez and Nagai (2020) in the Hyuga Nada Sea. Furthermore, when the LM develops, the large cyclonic meandering at the LM may provide a westward counter current near the coast. When this counter current becomes strong, the negative PV can be generated on the continental slope of the south coast of Honshu. Within the cyclonic meander of the LM, nutricline is expected to have a doming structure similar to the isopycnal doming in a cyclonic eddy. These turbulence generation mechanisms near the Kuroshio could, therefore, inject the domed nutrients in the LM to the sunlit surface layers (**Figure 10**).

The doming of the nutricline seen near the center of a cyclonic eddy can be more susceptible to the upper layer mixing and entrainment, that may supply domed nutrients to the euphotic zone. If this is the dominant cause of the phytoplankton increase during the LM, then the enhanced chlorophyll-a concentrations should occur at the center of the cyclonic circulation of the LM. However, the clear positive chlorophyll-a anomaly signal appears on the western side of the LM. In addition to the mesoscale doming of the nutrients in the cyclonic meander of the LM, submesoscale vertical motions can drive the localized injection of nutrients into the euphotic layer. The vertical motion associated with submesoscale dynamics is much stronger than that associated with mesoscale dynamics (Mahadevan and Tandon, 2006; Capet et al., 2008a,b; Lévy et al., 2012; McWilliams, 2016; Brannigan et al., 2017; Guo

et al., 2019) and could induce changes in phytoplankton growth or biomass (Martin and Richards, 2001; Klein and Lapeyre, 2009). As the small trigger meander is also a cyclonic eddy with the scale in the range of submesoscale, the nutrient could be supplied also through these submesoscale processes to the euphotic zone.

Recent studies have shown that the growth of instabilities within the mixed layer can tap potential energy of the mixed layer front to develop energetic submesoscale eddies, initially 1–10 km in horizontal extent and as deep as the ML. These eddies drive net horizontal transfer of lighter water above heavier water that can stratify the ML on a time scale of days to weeks. In addition, the eddy-driven restratification is important for light-limited phytoplankton to bloom at high latitude ocean fronts (Boccaletti et al., 2007; Fox-Kemper and Ferrari, 2008; Taylor and Ferrari, 2011; Mahadevan et al., 2012). This causes the surface sunlit layer to retain phytoplankton for longer periods, promoting a phytoplankton bloom. The Critical Depth Hypothesis (Sverdrup, 1953) posits out that vernal phytoplankton blooms occur when surface mixed layer depth shoals to a depth shallower than a critical depth at which integrated phytoplankton growth exceeds losses when nutrients are sufficient, and phytoplankton distribute homogeneously in the mixed layer. A deep MLD transports more phytoplankton to the dark subsurface layers, which does not allow them to grow with no light. On the other hand, when nutrients are not sufficient, the deeper mixed layer may increase the nutrients in sunlit layers, which would increase the phytoplankton; this is the case in autumn bloom. Therefore, the coincidence of chlorophyll-a positive anomaly with the shallower mixed layer during the Large Meander implies that the former phytoplankton increase mechanism caused by the re-stratification could be effective.

Our analysis on the MLD anomaly shows that the negative MLD anomaly is found in the LM with the positive chlorophyll-a anomaly during both the LM periods. However, for the occurrence of the phytoplankton increase caused by mixed layer restratification, nutrients need to be sufficient and the light has to be a major limiting factor for their growth. Because there is the mesoscale nutrient doming in the LM with several smaller scale nutrient injection mechanisms, such as the submesoscale vertical motions, and enhanced turbulence near the Kuroshio, the shallower MLD accompanied by the higher chlorophyll-a supports the hypothesis that the mixed layer re-stratification is also important for the formation of positive chlorophyll-a anomaly along the front in the LM (**Figure 10**). The satellite images during the current LM show that the higher concentration of chlorophyll-a on the western side of the LM with submesoscale chlorophyll filaments (**Supplementary Figure 4B**) and wiggles (**Supplementary Figure 4A**), consistent with the above notion.

The MLD anomalies for both the positive and negative signs seem to be intensified during autumn to spring (**Figure 7**). Although this is caused just by a fact that the deeper MLD during these seasons could have induced larger anomalies, these seasons are consistent with the submesoscale favorable seasons (Sasaki et al., 2014). Therefore, the coincidence of chlorophyll-a positive anomaly with the shallower mixed layer during the Large Meander implies that the former phytoplankton increase mechanism caused by the restratification could be effective.

The variations of phytoplankton community structures between LM and NLM have yet to be known. A study by Hidaka and Nakata (2010) reported that the interannual variations in the plankton ecosystem regarding sea surface chlorophyll and copepod biomass is attributed to local temperature and/or variation in surface irradiance. Besides, the phytoplankton distribution and biological production in coastal waters depend primarily on the nutrient availability in the euphotic zone. Near the Izu Peninsula the dominant phytoplankters are the diatoms in particular *Chaetoceros* spp. in September 1980 (Takahashi and Kishi, 1984).

5. SUMMARY AND CONCLUSIONS

In this study, the influence of the Kuroshio Large Meander (LM) on the surface chlorophyll-a concentration is investigated using the satellite chlorophyll-a data from 1997 to January 2019. We found for the first time that during large meander periods the positive chlorophyll-a anomaly appears along the Kuroshio from the regions south of Kyushu and Cape Shiono-Misaki to the southernmost part of the LM off Enshu-Nada. The positive chlorophyll-a anomaly during the LM periods coincides with the shallower mixed layer depth (MLD), implying that mixed layer re-stratification caused by submesoscale flows along the Kuroshio could be effective to support phytoplankton growth. During the course of the LM events, the positive chlorophyll-a anomaly appears first in the region south of Kyushu within the small cyclonic meander on the coast side of the Kuroshio front. This cyclonic meander, known as the trigger meander of the LM, slowly propagates toward the downstream retaining the positive chlorophyll-a anomaly, which then reaches the LM region. As this small meander has the cyclonic circulation characters, nutrients doming structures are expected. The domed nutricline can be more susceptible to the stirring and mixing processes in the upper layers, such as the submesoscale upwelling, and microscale turbulent mixing, both of which are known to be enhanced at ocean fronts (Mahadevan and Tandon, 2006; Nagai et al., 2009, 2012, 2017, 2019a,b, 2021; D'Asaro et al., 2011). Although it is contradict to the previous results (Kawabe, 1987), our results show that the distance between the Kuroshio and the southeastern coast of Kyushu decreases during the LM periods. The closely flowing Kuroshio to the continental slope in the upstream region may induce the strong turbulence, which keeps supplying nutrients to the downstream regions (Nagai et al., 2019a; Durán Gómez and Nagai, 2020).

The enhanced chlorophyll-a concentration during the LM periods on the western part of the LM along the Kuroshio could play an important role for the higher trophic levels. However, it still remains unclear how the positive chlorophyll-a anomaly is formed right at the LM region. Intensive multidisciplinary observations to measure turbulence,

high-resolution three-dimensional density structures, nutrient concentrations, and abundance and community structures of primary and secondary producers are required to understand the cause and influences of the enhanced chlorophyll-a in the LM.

DATA AVAILABILITY STATEMENT

Publicly available datasets were analyzed in this study. This data can be found at: https://marine.copernicus.eu/.

AUTHOR CONTRIBUTIONS

DALB analyzed the satellite data and provided the figures of the paper. RCS, TN, and TH assisted the analyses. DALB provided the first draft of the manuscript. DALB, RCS, TN, and TH edited the manuscripts. All authors contributed to the article and approved the submitted version.

ACKNOWLEDGMENTS

TN and DALB thank SKED (JPMXD0511102330). TN and RCS thank OMIX (KAKENHI16H01590 and 18H04914) and KAKENHI (19H01965). TN, DALB, and RCS thank continuous support from the pAnTS project.

SUPPLEMENTARY MATERIAL

The Supplementary Material for this article can be found online at: https://www.frontiersin.org/articles/10.3389/fmars.2021.677632/full#supplementary-material

REFERENCES

Akitomo, K., Awaji, T., and Imasato, N. (1991). Kuroshio path variation south of Japan. Part 1: barotropic inflow-outflow model. *J. Geophys. Res.* 96, 2549–2560. doi: 10.1029/90JC02030

Ambe, D., Endoh, T., Hibiya, T., and Imawaki, S. (2009). Transition to the large meander path of the Kuroshio as observed by satellite altimetry. *Mer* 47, 19–27.

Ambe, D., Imawaki, S., Uchida, H., and Ichikawa, K. (2004). Estimating the Kuroshio axis south of Japan using combination of satellite altimetry and drifting buoys. *J. Phys. Oceanogr.* 60, 375–382. doi: 10.1023/B:JOCE.0000038343.31468.fe

Bocaletti, G., Ferrari, R., and Fox-Kemper, B. (2007). Mixed layer instabilities and restratification. *J. Phys. Oceanogr.* 37, 2228–2250. doi: 10.1175/JPO3101.1

Brannigan, L., Marshall, D. P., Naveira Garabato, A., Nurser, G., and Kaiser, J. (2017). Submesoscale instabilities in mesoscale eddies. *J. Phys. Oceanogr.* 47, 3061–3085. doi: 10.1175/JPO-D-16-0178.1

Capet, X., McWilliams, J. C., Molemaker, M. J., and Shchepetkin, A. F. (2008a). Mesoscale to submesoscale transition in the California Current System. Part II: Frontal processes. *J. Phys. Oceanogr.* 38, 44–64. doi: 10.1175/2007JPO3672.1

Capet, X., McWilliams, J. C., Molemaker, M. J., and Shchepetkin, A. F. (2008b). Submesoscale transition in the California Current system. Part I: Flow structure, eddy flux, and observational tests. *J. Phys. Oceanogr.* 38, 29–43. doi: 10.1175/2007JPO3671.1

Chao, S. Y. (1984). Bimodality of the Kuroshio. *J. Phys. Oceanogr.* 14, 92–103. doi: 10.1175/1520-0485(1984)014<0092:BOTK>2.0.CO;2

D'Asaro, E., Lee, C., Rainville, L., Harcourt, L., and Thomas, L. (2011). Enhanced turbulence and energy dissipation at ocean fronts. *Science* 332, 318–322. doi: 10.1126/science.1201515

Durán Gómez, G. S., and Nagai, T. (2020). "Elevated nutrient supply caused by the kuroshio approaching to the continental shelf associated with submesoscale flows and near-inertial waves," in *Fall Meeting, AGU Presented at 2020* (San Francisco, CA).

Ebuchi, N., and Hanawa, K. (2000). Mesoscale eddies observed by TOLEX-ADCP and TOPEX/POSEIDON altimeter in the Kuroshio recirculation region south of Japan. *J. Oceanogr.* 56, 43–57.

Ebuchi, N., and Hanawa, K. (2003). Influence of mesoscale eddies on variations of the Kuroshio path south of Japan. *J. Oceanogr.* 59, 25–36. doi: 10.1023/A:1022856122033

Endoh, T., and Hibiya, T. (2000). Numerical study of the generation and propagation of trigger meanders of the Kuroshio south of Japan. *J. Oceanogr.* 56, 409–418. doi: 10.1023/A:1011176322166

Endoh, T., and Hibiya, T. (2001). Numerical simulation of the transient response of the kuroshio leading to the large meander formation south of Japan. *J. Geophys. Res.* 106, 26833–26850. doi: 10.1029/2000JC000776

Endoh, T., and Hibiya, T. (2009). Interaction between the trigger meander of the Kuroshio and the abyssal anticyclone over Koshu Seamount as seen in the reanalysis data. *Geophys. Res. Lett.* 36:L18604. doi: 10.1029/2009GL039389

Fox-Kemper, B., and Ferrari, R. (2008). Parameterization of mixed layer eddies. Part II: prognosis and impact. *J. Phys. Oceanogr.* 38, 1166–1179. doi: 10.1175/2007JPO3788.1

Gula, J., Molemaker, M. J., and McWilliams, J. (2016). Submesoscale dynamics of a Gulf Stream frontal eddy in the South Atlantic Bight. *J. Phys. Oceanogr.* 46, 305–325. doi: 10.1175/JPO-D-14-0258.1

Guo, M., Xiu, P., Chai, F., and Xue, H. (2019). Mesoscale and submesoscale contributions to high sea surface chlorophyll in subtropical gyres. *Geophys. Res. Lett.* 46, 13217–13226. doi: 10.1029/2019GL085278

Hayasaki, M., Kawamura, R., Mori, M., and Watanabe, M. (2013). Response of extratropical cyclone activity to the Kuroshio large meander in northern winter. *Geophys. Res. Lett.* 40, 2851–2855. doi: 10.1002/grl.50546

Hidaka, K., and Nakata, K. (2010). Interannual variations of the planktonic ecosystem in the slope water and Kuroshio south of Japan in February in the years 1990–2002. *J. Oceanogr.* 66, 741–753. doi: 10.1007/s10872-010-0061-5

Ichikawa, K. (2001). Variation of the Kuroshio in the Tokara Strait induced by meso-scale eddies. *J. Oceanogr.* 57, 55–68. doi: 10.1023/A:1011174720390

Kagimoto, T., Miyazawa, Y., Guo, X., and Kawajiri, H. (2008). "High resolution Kuroshio forecast system: description and its applications," in *High Resolution Numerical Modelling of the Atmosphere and Ocean,* eds K. Hamilton and W. Ohfuchi (New York, NY: Springer).

Kawabe, M. (1985). Sea level variations at the Izu Islands and typical stable paths of the Kuroshio. *J. Oceanogr. Soc. Jpn.* 41, 307–326. doi: 10.1007/BF02109238

Kawabe, M. (1986). Transition processes between the three typical paths of the Kuroshio. *J. Oceanogr. Soc. Jpn.* 42, 174–191. doi: 10.1007/BF02109352

Kawabe, M. (1987). Spectral properties of sea level and time scales of Kuroshio path variations. *J. Oceanogr. Soc. Jpn.* 43, 111–123. doi: 10.1007/BF02111887

Kawabe, M. (1995). Variations of current path, velocity, and volume transport of the Kuroshio in relation with the large meander. *J. Phys. Oceanogr.* 25, 3103–3117. doi: 10.1175/1520-0485(1995)025<3103:VOCPVA>2.0.CO;2

Kimura, S., Kasai, A., Nakata, H., Sugimoto, T., Simpson, J. H., and Cheok, J. V. S. (1997). Biological productivity of meso-scale eddies caused by frontal disturbances in the Kuroshio. *ICES J. Mar. Sci.* 54, 179–192.

Klein, P., and Lapeyre, G. (2009). The oceanic vertical pump induced by mesoscale and submesoscale turbulence. *Annu. Rev. Mar. Sci.* 1, 351–375. doi: 10.1146/annurev.marine.010908.163704

Lévy, M., Iovino, D., Resplandy, L., Klein, P., Madec, G., Tréguier, A.-M., et al. (2012). Large-scale impacts of submesoscale dynamics on phytoplankton: local and remote effects. *Ocean Model.* 43, 77–93. doi: 10.1016/j.ocemod.2011.12.003

Liu, X., Mu, M., and Wang, Q. (2018). The nonlinear optimal triggering perturbation of the Kuroshio large meander and its evolution in a regional ocean model. *J. Phys. Oceanogr.* 48, 1771–1786. doi: 10.1175/JPO-D-17-0246.1

Mahadevan, A., D'Asaro, E., Lee, C., and Perry, M. J. (2012). Eddy-driven stratification initiates North Atlantic spring phytoplankton blooms. *Science* 337, 54–58. doi: 10.1126/science.1218740

Mahadevan, A., and Tandon, A. (2006). An analysis of mechanisms for submesoscale vertical motion at ocean fronts. *Ocean Model.* 14, 241–256. doi: 10.1016/j.ocemod.2006.05.006

Martin, A. P., and Richards, K. J. (2001). Mechanisms for vertical nutrient transport within a North Atlantic mesoscale eddy. *Deep Sea Res. Part II Top. Stud. Oceanogr.* 48, 757–773. doi: 10.1016/S0967-0645(00)00096-5

Masuda, A. (1982). An interpretation of the bimodal character of the stable Kuroshio path. *Deep Sea Res. Part A Oceanogr. Res. Pap.* 29, 471–484. doi: 10.1016/0198-0149(82)90071-1

McWilliams, J. C. (2016). Submesoscale currents in the ocean. *Proc. R. Soc. A Math. Phys. Eng. Sci.* 472:20160117. doi: 10.1098/rspa.2016.0117

Mitsudera, H., Waseda, T., Yoshikawa, Y., and Taguchi, B. (2001). Anticyclonic eddies and Kuroshio meander formation. *Geophys. Res. Lett.* 28, 2025–2028. doi: 10.1029/2000GL012668

Miyazawa, Y., Guo, X., and Yamagata, T. (2004). Roles of mesoscale eddies in the Kuroshio paths. *J. Phys. Oceanogr.* 34, 2203–2222. doi: 10.1175/1520-0485(2004)034<2203:ROMEIT>2.0.CO;2

Miyazawa, Y., Kagimoto, T., Guo, X., and Sakuma, H. (2008). The Kuroshio large meander formation in 2004 analyzed by an eddy-resolving ocean forecast system. *J. Geophys. Res.* 113:C10015. doi: 10.1029/2007JC004226

Miyazawa, Y., Yamane, S., Guo, X., and Yamagata, T. (2005). Ensemble forecast of the Kuroshio meandering. *J. Geophys. Res.* 110:C10026. doi: 10.1029/2004JC002426

Nagai, T., Clayton, S., and Uchiyama, Y. (2019b). "Multiscale routes to supply nutrients through the kuroshio nutrient stream," in *Kuroshio Current,* eds T. Nagai, H. Saito, K. Suzuki, and M. Takahashi.

Nagai, T., Durán Gómez, G. S., Otero, D. A., Mori, Y., Yoshie, N., Ohgi, K., et al. (2019a). How the Kuroshio Current delivers nutrients to sunlit layers on the continental shelves with aid of near-inertial waves and turbulence. *Geophys. Res. Lett.* 46, 6726–6735. doi: 10.1029/2019GL082680

Nagai, T., Hasegawa, D., Tanaka, T., Nakamura, H., Tsutsumi, E., Inoue, R., et al. (2017). First evidence of coherent bands of strong turbulent layers associated with high-wavenumber internal- wave shear in the upstream Kuroshio. *Sci. Rep.* 7:14555. doi: 10.1038/s41598-017-15167-1

Nagai, T., Rosales Quintana, G. M., Durán Gómez, G. S., Hashihama, F., and Komatsu, K. (2021). Elevated turbulent and double-diffusive nutrient flux in the kuroshio over the Izu Ridge and in the Kuroshio Extension. *J. Oceanogr.* 77, 55–74. doi: 10.1007/s10872-020-00582-2

Nagai, T., Tandon, A., Yamazaki, H., and Doubell, M. J. (2009). Evidence of enhanced turbulent dissipation in the frontogenetic Kuroshio Front thermocline. *Geophys. Res. Lett.* 36:L12609. doi: 10.1029/2009GL038832

Nagai, T., Tandon, A., Yamazaki, H., Doubell, M. J., and Gallager, S. (2012). Direct observations of microscale turbulence and thermohaline structure in the Kuroshio Front. *J. Geophys. Res.* 117:C08013. doi: 10.1029/2011JC007228

Nagano, A., Yamashita, Y., Hasegawa, T., Ariyoshi, K., Matsumoto, H., and Shinohara, M. (2018). Characteristics of an atypical large-meander path of the Kuroshio Current south of Japan formed in september 2017. *Mar. Geophys. Res.* 40, 525–539. doi: 10.1007/s11001-018-9372-5

Nakamura, H., Nishina, A., and Minobe, S. (2012). Response of storm tracks to bimodal Kuroshio path states south of Japan. *J. Clim.* 25, 7772–7779. doi: 10.1175/JCLI-D-12-00326.1

Nakata, K. (1994). Variations in food abundance for Japanese sardine larvae related to the Kuroshio meander. *Fish. Oceanogr.* 3, 39–49. doi: 10.1111/j.1365-2419.1994.tb00046.x

Qiu, B., and Chen, S. (2005). Variability of the Kuroshio Extension jet, recirculation gyre, and mesoscale eddies on decadal time scales. *J. Phys. Oceanogr.* 35, 2090–2103. doi: 10.1175/JPO2807.1

Sasaki, H., Klein, P., Qiu, B., and Sasai, Y. (2014). Impact of oceanic-scale interactions on the seasonal modulation of ocean dynamics by the atmosphere. *Nat. Commun.* 5:6636. doi: 10.1038/ncomms6636

Solomon, H. (1978). Occurrence of small "trigger meanders" in the Kuroshio off southern kyushu. *J. Oceanogr. Soci. Jpn.* 34, 81–84.

Stommel, H., and Yoshida, K. (1972). *Kuroshio: Its Physical Aspects.* Tokyo: University of Tokyo Press.

Sverdrup, H. (1953). On conditions for the vernal blooming of phytoplankton. *J. Conseil Permanent Int. l'Explor.* 18, 287–295.

Taft, B. A. (1972). "Characteristics of the flow of the Kuroshio south of Japan," in *Kuroshio-Its Physical Aspects,* eds H. Stommel and K. Yoshida (University of Tokyo Press), 165–216.

Takahashi, M., and Kishi, M. J. (1984). Phytoplankton growth response to wind induced regional upwelling occurring around the Izu islands off Japan. *J. Oceanogr. Soc. Jpn.* 40, 221–229. doi: 10.1007/BF02302556

Taylor, J. R., and Ferrari, R. (2011). Ocean fronts trigger high latitude phytoplankton blooms. Geophys. Res. Lett. 38:L23601. doi: 10.1029/2011GL049312

Uda, M. (1937). On the recent abnormal condition of the Kuroshio to the south of Kii Peninsula, (in Japanese). *Kagaku* 7, 360–361.

Usui, N. (2019). "Progress of studies on Kuroshio path variations south of Japan in the past decade," in *Kuroshio Current,* eds T. Nagai, H. Saito, K. Suzuki, and M. Takahashi.

Usui, N., Tsujino, H., Fujii, Y., and Kamachi, M. (2008). Generation of a trigger meander for the 2004 Kuroshio large meander. *J. Geophys. Res.* 113:C01012. doi: 10.1029/2007JC004266

Usui, N., Tsujino, H., Nakano, S., and Matsumoto, S. (2013). Long-term variability of the Kuroshio path south of Japan. *J. Oceanogr.* 69, 647–670. doi: 10.1007/s10872-013-0197-1

Waseda, T., Mitsudera, H., Taguchi, B., and Yoshikawa, Y. (2002). On the eddy-Kuroshio interaction: evolution of the mesoscale eddy. *J. Geophys. Res.* 107, 3–1–3–19. doi: 10.1029/2000JC000756

White, W. B., and McCreary, J. P. (1976). On the formation of the Kuroshio meander and its relationship to the large-scale ocean circulation. *Deep-Sea Res.* 23, 33–47. doi: 10.1016/0011-7471(76)90806-8

Xu, H., Tokinaga, H., and Xie, S.-P. (2010). Atmospheric effects of the Kuroshio large meander during 2004–05. *J. Clim.* 23, 4704–4715. doi: 10.1175/2010JCLI3267.1

Yamada, K., Ishizaka, J., Yoo, S., cheol Kim, H., and Chiba, S. (2004). Seasonal and interannual variability of sea surface chlorophyll a concentration in the Japan/East sea (JES). *Prog. Oceanogr.* 61, 193–211. doi: 10.1016/j.pocean.2004.06.001

Yasuda, I., Yoon, J. H., and Suginohara, N. (1985). Dynamics of the Kuroshio large meander-barotropic model. *J. Oceanogr. Soc. Jpn.* 48, 259–273. doi: 10.1007/BF02109275

Conflict of Interest: The authors declare that the research was conducted in the absence of any commercial or financial relationships that could be construed as a potential conflict of interest.

The handling editor declared a past collaboration with one of the authors, TN.